Proximitized insulators from disordered superconductors

Moshe Haim [1,2] David Dentelski [1] and Aviad Frydman [1]
[1]*Department of Physics, Jack and Pearl Resnick Institute and the Institute of Nanotechnology and Advanced Materials, Bar-Ilan University, Ramat-Gan 52900, Israel*
[2]*Department of Condensed Matter Physics, Weizmann Institute of Science, Rehovot 76100, Israel*

(Received 31 July 2022; revised 7 June 2023; accepted 10 July 2023; published 20 July 2023)

We present an experimental study of bilayers of a disordered Ag metal layer close to the metal-insulator transition and an indium-oxide film which is on the insulating side of the superconductor insulator transition. Our results show that superconducting fluctuations within the indium-oxide film, that proximitize the underlying metal layer, induce *insulating* rather than superconducting behavior. This is ascribed to suppression of density of states (due to the superconducting energy gap) for quasiparticles in the proximitized regions. Our results present a manifestation of the proximity effect phenomenon and provide important insight into the nature of the insulating phase of the disorder driven superconductor insulator transition.

DOI: 10.1103/PhysRevB.108.014505

I. INTRODUCTION

The interplay between superconductivity and disorder is a very active topic of investigation. It was recognized decades ago that *s*-wave superconductivity is remarkably robust against weak disorder [1]. The situation is different for strong disorder. Experiments show that superconductivity in two-dimensional (2D) films can be destroyed by strong enough disorder as well as other nonthermal tuning parameters, *g*, such as magnetic field, thickness, chemical composition, gate voltage, and pressure [2–33]. Once superconductivity is destroyed, the system undergoes a transition to an insulating state (for reviews see [34,35]). This superconductor-insulator-transition (SIT) is a paradigmatic example for a quantum phase transition that can occur in systems driven by a nonthermal tuning parameter [36].

One of the ongoing deliberations in the field of the SIT is the nature of the insulating phase, I_S. It has been shown both theoretically [37–40] and experimentally [41] that in some nominally *s*-wave BCS superconductors, the presence of disorder can separate the temperature T^* where pairing occurs accompanied by the development of an energy gap in the local density of states [16,42], and the actual T_c where the superfluid density becomes finite. The pseudogap region between these temperatures grows with disorder as the SIT is approached and eventually, in the insulating regime, a finite superconducting gap, Δ, exists even in the absence of superfluid density. Indeed, similar energy gap [41] (as well as vortex motion [17,43] and Nernst signals [18]) were measured in both the superconductor and I_S phases of disordered films. These results led to the realization that a BCS superconductor can undergo a quantum phase transition to an insulating phase of bosons rather than unpaired electrons. Hence I_S, which is composed of uncorrelated superconducting fluctuations, shows a number of properties similar to those of a bulk superconductor despite being an electrical insulator. In this article, we study a special aspect of the superconducting nature of I_S, i.e., the proximity effect to a normal metal.

The classic proximity effect describes the mutual influence of two "clean" layers—one is a superconductor, *SC*, and one is a normal metal, *N*, placed in a good electric contact, resulting in the induction of finite superconductivity into the *N* and suppression of the superconducting order parameter in the *SC* [44,45]. Experiments have shown [46,47] that, when the superconductor is highly disordered, superconducting quantum fluctuations (even within the I_S) can induce superconductivity into a proximitized *N*. In this article we report on a more exotic effect which occurs when the *N* is highly disordered so that it is close to the metal insulator transition. Our main results are the following.

(1) Placing a highly disordered metal in proximity to an I_S can induce *insulating* behavior in the *N*.

(2) This effect becomes more prominent as the I_S is driven towards the SIT.

(3) The effect is larger the more disordered is the *N* layer.

We provide a simple model to explain these results based on enhanced electronic localization in the disordered metal due to proximitized superconducting fluctuations in the normal region.

II. EXPERIMENTAL

The samples for this study were prepared using the following scheme. Six Au leads were deposited on an insulating SiO substrate [gold pads in Fig. 1(a)]. Then, two 10 nm thick Ag strips were deposited between two sets of leads, to be used as the *N* proximity layer [gray strips in Fig. 1(a)]. In order to increase the disorder of the silver, the samples were thinned in an Ar plasma chamber in short pulses for different amounts of time. Here we present results for three highly disordered Ag films, S1, S2, and S3, having decreasing Ag room temperature sheet resistances of 250, 220, and 150 $\Omega_{\square}$, respectively. Finally, a 30 nm thick layer of amorphous indium oxide (InO) was e-beam deposited in a 10^{-4} mbar partial oxygen pressure resulting in a highly disordered, insulating film [purple layer

 ©2023 American Physical Society

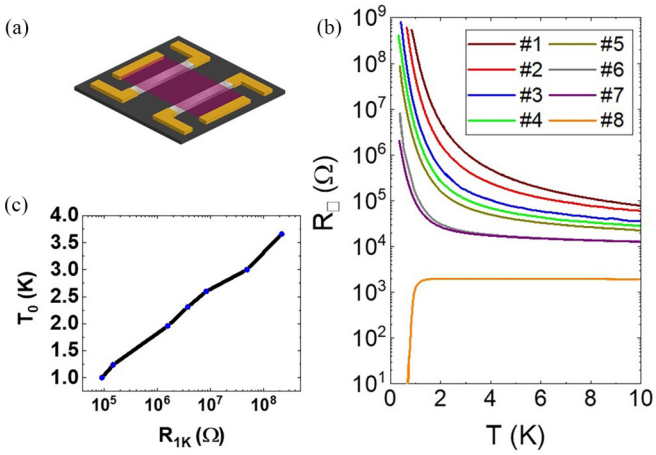

FIG. 1. (a) Sketch of the device containing six leads (gold), two silver strips (gray), and the InO layer (purple). (b) Resistance vs temperature of the InO layer of sample S1, for different stages of annealing (as noted in the legend), measured between the silver strips. (c) T_0 (extracted from the $R = R_0 e^{\frac{T_0}{T}}$ dependency) vs the 1 K InO sheet resistance. The black line is a guide to the eye.

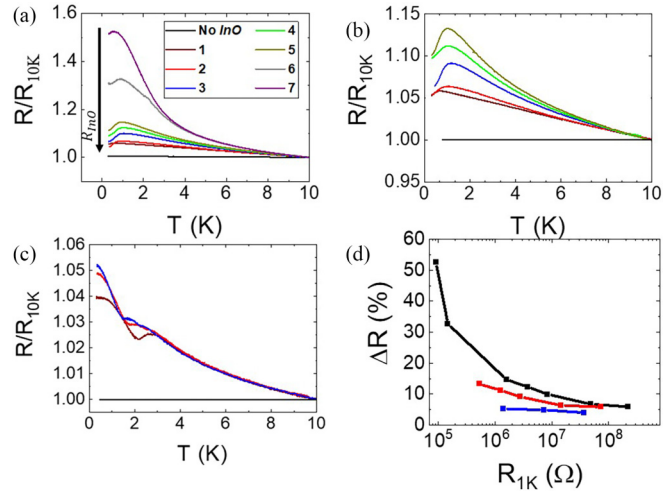

FIG. 2. Resistance vs temperature of the three Ag/InO bilayer of samples S1, S2, and S3 [panels (a), (b), and (c), respectively], for different stages of annealing. The colors signaling the annealing stage (see legend) apply for S2 and S3 as well; however, the sheet resistances of the InO film may differ between the samples. Black lines are plots for the bare Ag films. For clarity, the curves are normalized to the resistance at 10 K. (d) Resistance maximum vs the InO resistance at 1 K of samples S1 (black), S2 (red), and S3 (blue).

in Fig. 1(a)]. The resistance of the InO film was sequentially reduced via low temperature thermal annealing, thus driving the film through the insulator to superconductor transition [18,48]. This setup takes advantage of the fact the Ag layer is significantly more conductive than the InO layer and allows one to use the Ag layer as a voltage terminal for four-probe resistance measurements of the bare InO film and two-probe measurements of the resistance of the Ag/InO bilayer as the InO is driven through the SIT.

III. RESULTS

InO films, despite being morphologically uniform [48,49], have been shown to include emergent granularity in the form of superconducting puddles embedded in an insulating matrix [18,41,43,50]. Hence local superconductivity is present even in the insulating phase of the SIT. Figure 1(b) shows the resistance vs temperature curves of the bare InO of S1 for different annealing stages (sequentially reducing $R_\square$). The insulating curves are found to follow $R = R_0 e^{T_0/T}$ behavior. This is a typical feature of I_S insulators, which are characterized by emergent granularity [15,51–53]. Figure 1(c) presents T_0 versus R of the InO film, which is found to decrease as the sample approaches the SIT and extrapolates to zero close to (but beyond) it, in consistence with previously reported works [15].

The key result of this work is presented in Fig. 2, which shows the resistance versus temperature curves for the three Ag/InO bilayers. As long as the InO is in the insulating phase, the resistance of such a bilayer is governed by the Ag layer, which has a much lower sheet resistance ($\approx 200\Omega_\square$) than that of the InO ($\approx 100k\Omega_\square - 100M\Omega_\square$) for $T \leqslant 10$ K. Thus, when measuring the bilayer, we are, in fact, measuring the Ag layer almost strictly. We note that the annealing process may slightly affect the Ag resistance as well.

We start with considering the results of sample S1 (having the highest Ag resistance) represented in Fig. 2(a). Surprisingly, the addition of InO causes the resistance to *increase* with decreasing temperature below ~10 K. This is very counterintuitive since one naively expects that the InO would add conductivity in parallel and, if anything, would reduce the total resistance. Instead, the InO overlayer seems to be inducing insulating behavior in the underlying Ag film. This effect gets larger as the InO is driven towards the SIT, eventually exceeding a 50% amplitude increase before reversing the trend at low temperatures where the resistance starts decreasing with lowering temperature.

A similar effect, though with smaller magnitude, was seen for samples S2 and S3, having decreasing disorder, respectively [Figs. 2(b) and 2(c)]. Figure 2(d) shows the peak amplitude versus $R_\square$ for the three samples, indicating that the resistance increase depends on two parameters. It is larger the more disordered the Ag film is and also the closer the InO is to the SIT.

IV. DISCUSSION AND NUMERICAL SIMULATIONS

In order to understand how inducing superconducting fluctuations in a N layer results in an increase of resistance we recall that our Ag films are highly disordered, close to being insulating themselves. The conductivity is thus inhomogeneous due to strong spatial fluctuations of the underlying electronic potential. The current does not flow uniformly through the sample but rather through preferred high conductance trajectories as illustrated in the conductivity map of Fig. 3(a).

Adding a disordered superconducting overlayer induces islands of *SC* regions in the Ag film [purple dots in Fig. 3(b)] at temperatures below T_c. As the temperature is lowered, the density of superconducting regions increases. However, when global phase coherence is absent, the insertion of superconducting islands into a highly disorder metal can actually

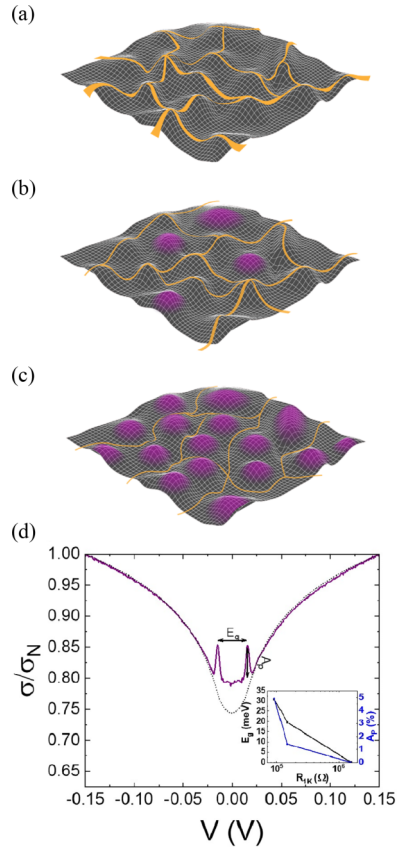

FIG. 3. Illustration of the current paths (in orange) through the Ag film. (a) The 2D conductivity map of the Ag film prior to the InO deposition. The current is carried by the most conductive parts (peaks in the 2D map). (b) Adding an InO layer proximitizes different parts of the Ag film and induces superconductivity, represented in purple. The current bypasses the SC regions due to suppression of the DOS in these locations. (c) Annealing the InO leads to more sections of the Ag being proximitized thus further limiting the current paths and forcing them to choose less conductive routes, thus further increasing the resistance. (d) Differential conductivity vs bias voltage of sample S1 for the last insulating stage, normalized to the data at 150 meV. The inset shows the relative peak height and energy separation for different disorder degrees.

increase the resistivity. This is due to the formation of a local energy gap, Δ, within each island, which suppresses the density of states for quasiparticles and thus limits the current flow through these islands. Because the regions that are more prone to the proximity process are, naturally, those with higher conductivity, the current is restricted to one of two options: flowing through the high resistance trajectories [Fig. 3(b)] or through the puddles of zero resistance, but at an energy "cost" of 2Δ. Therefore, the sample can be viewed as a network of SIS junctions where the experimentally observed gap overlays the individual local ones which the current must tunnel through. A similar process was suggested as the origin for the giant magnetoresistance peak observed in these materials at high fields and low temperatures [54,55].

Lowering the disorder of the *SC* and pushing it towards the SIT (e.g., by annealing the InO layer) increases the density of superconducting puddles [Fig. 3(c)], thus further limiting the current carrying network and forcing the current to flow through higher resistance trajectories. This results in increasing the bilayer resistivity as the InO film is pushed towards the SIT as indeed seen in the experiment [Fig. 2(d)]. In addition, reducing the N disorder smooths the potential background, thus suppressing the above process.

The temperature onset of this unique proximity effect is $\sim$10 K, which is significantly larger than the maximal T_c measured in InO films ($\sim$3.5 K [18]). However, STM measurements on a film of InO with $T_C \approx 3$ K have detected a finite Δ up to temperatures of $\approx$6.5 K [16]. In the insulator, Δ is predicted to grow further and increase as disorder increases [39]. The real pairing critical temperature, T^*, of the I_s phase of InO is yet unknown, but the results presented here show signs for superconductivity up to $T \approx 10$ K.

The schematic representation of the current flow through the Ag layer in Figs. 3(a)–3(c) is modeled here by considering an $L \times L$ squared lattice, where each site can be either a superconductor or a normal metal. We consider only nearest neighbors connections and assign a resistance $r = 1$ for each bond between two metallic sites. The total sheet resistance, $R_\square$, is then calculated by the minimal resistance path required for the current to flow from one side of the bilayer to the other normalized by the size of the lattice. This is to say, that for $t = \frac{T}{T_c} \geqslant 1$, where all sites are metallic, $R_\square = 1$.

With decreasing temperature, proximitized superconducting islands start to form in the Ag layer. This is manifested by reweighting all the bonds' resistances connecting a superconducting site to a metallic one by a factor $Z \geqslant 1$, while all bonds between two neighboring superconducting sites (within a SC island) are assigned a resistance $r = 0$, such that $R_\square \to 0$ as the superconducting density, n_{sc}, becomes large. The different sites are chosen randomly to be metallic or superconductors, depending on the value of $n_{sc}(t) \in [0, 1]$.

We include the effect of disorder by introducing sites in the normal metal that prevent the formation of superconductivity. We assign a resistance $r(t) = r_0 e^{T_0/T}$ between a site within a superconducting or a metal region to a disordered one. Here, we use $r_0 = \exp(-1)$ and $T_0 = 1.05T_c$, such that the high-temperature resistivity of the different samples is $\approx$5% higher than the clean one. The strength of the disorder is defined by the density of these sites, N_d.

Figure 4(a) shows the resistance as a function of the reduced temperature t for a fixed value of N_d and different values of Z, where we used the empirical approximate temperature dependence of the superconducting fraction: $n_{sc}(t) = 1 - t^{0.4}$. For all values of disorder, decreasing the temperature increases the density of superconducting islands and hence increases $R_\square$. This trend continues down to a disorder-dependent temperature, which marks the onset of global superconductivity, thus leading to the peak in the R-T curve, as is found in the experiments. Note that the broad transition is also consistent with the experimental results. Figure 4(b) shows the results for constant $Z = 3$ and different degrees of disorder, N_d. It is seen that, as the disorder increases, the resistivity peak is found to be higher as indeed observed in the experiments.

The above picture is strongly supported by the differential conductance curve shown in Fig. 3(d), which resembles an insulating stage of S1. The overall dI/dV versus V curve

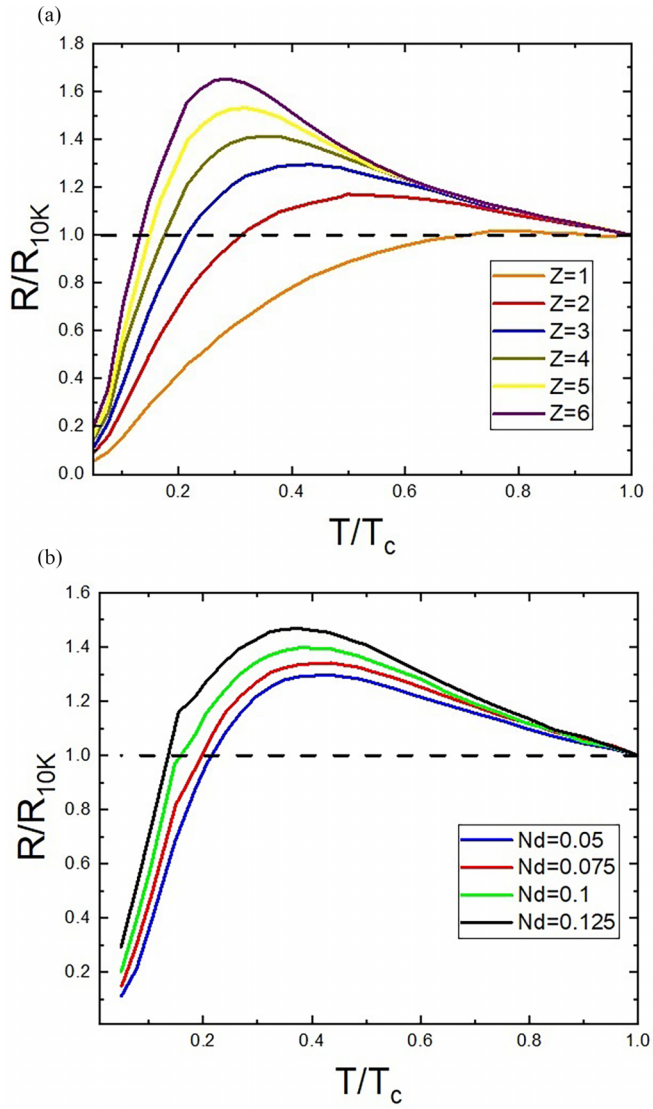

FIG. 4. Normalized sheet resistance $R_{\square}(t)$ of an $L = 50$ squared lattice normalized by its value at T_c, as a function of the reduced temperature $t = T/T_c$. (a) Fixed disorder density $N_d = 0.05$ for different values of Z. As the temperature decreases, there is an interplay between the gain of a current passing through a zero-resistance superconducting island and the cost, Z, to enter and exit the island. (b) Fixed $Z = 3$ for samples with different disorder density, N_d. The dashed lines mark the sheet resistance at $T = T_c$.

exhibits a suppression of conductance as the bias voltage is lowered, due to the Altshuler-Aronov (AA) mechanism of electron-electron interactions [56] in the disordered Ag film (dashed curve). At low bias, the curve exhibits a superimposed structure which includes two symmetrical maxima that resemble the coherence peaks of a superconducting gap structure. The peak amplitude and energy scale grow as the sample is further annealed and pushed towards the SIT; however, they are only observed in the most disordered Ag film (S1) and when the overlayer InO film is close to the SIT, as seen in the inset. The energy scales extracted from these features are 19.6 and 30.8 meV for the two last insulating InO stages. Interestingly, these are integer multiples (14 and 22, respectively) of 1.4 meV, which is the value of 2Δ for amorphous InO [41]. This is consistent with the suggested model of current flowing through a series of *SIS* junctions giving rise to a global gaplike structure, which is the sum of the individual local gaps on each of the SC islands and is superimposed on the AA trend.

V. SUMMARY

The results presented in this paper demonstrate a different type of proximity effect. We show that inducing superconductivity into an N layer is not limited to "clean" superconductors but can also be extended to an I_S phase. Moreover, in the case of a highly disordered N, the proximity of a disordered metal to the I_S can induce insulating-like behavior, thus reducing its conductance. This effect becomes more prominent the larger the N disorder. Such a proximitized bilayer can also offer a useful tool to study the I_S deep into the insulating phase. Attempting to measure superconducting fluctuations in an insulating sample by transport is ineffective, since the exponentially increasing resistance screens local superconductivity. Tunneling measurement requires a barrier that is much more resistive than the sample itself, limiting the measurement to samples that are close to the transition and at relatively high temperatures. Contrarily, by coupling a film that is well within the insulating phase of the SIT to a normal metal, one can access a transport and tunneling measurement of the coupled metal, regardless of how insulating the superconductor is. The interplay between the metal and the superconductor is quantified in our numerical model as a single parameter denoted as Z, which can be extracted directly from simple tunneling measurements and can be studied for different samples and materials.

ACKNOWLEDGMENTS

We are grateful for technical help from I. Volotsenko, R. Cohen, Y. Stein, A. Fried, A. Roy, and M. Laav and useful discussions with J. Ruhman, N. Trivedi, and T. Baturina. This work was supported by the US-Israel Bi-national Science Foundation (BSF) Grant No. 2020331.

[1] P. W. Anderson, Absence of diffusion in certain random lattices, Phys. Rev. **109**, 1492 (1958).
[2] M. Strongin, R. S. Thompson, O. F. Kammerer, and J. E. Crow, Destruction of superconductivity in disordered near-monolayer films, Phys. Rev. B **1**, 1078 (1970).
[3] R. C. Dynes, A. E. White, J. M. Graybeal, and J. P. Garno, Breakdown of Eliashberg Theory for Two-Dimensional Superconductivity in the Presence of Disorder, Phys. Rev. Lett. **57**, 2195 (1986).
[4] D. B. Haviland, Y. Liu, and A. M. Goldman, Onset of Superconductivity in the Two-Dimensional Limit, Phys. Rev. Lett. **62**, 2180 (1989).
[5] J. M. Valles, Jr., R. C. Dynes, and J. P. Garno, Electron Tunneling Determination of the Order-Parameter Amplitude at the

Superconductor-Insulator Transition in 2D, Phys. Rev. Lett. **69**, 3567 (1992).

[6] A. Frydman, O. Naaman, and R. C. Dynes, Universal transport in two-dimensional granular superconductors, Phys. Rev. B **66**, 052509 (2002).

[7] H. Aubin, C. A. Marrache-Kikuchi, A. Pourret, K. Behnia, L. Bergé, L. Dumoulin, and J. Lesueur, Magnetic-field-induced quantum superconductor-insulator transition in $Nb_{0.15}Si_{0.85}$, Phys. Rev. B **73**, 094521 (2006).

[8] M. D. Stewart, Jr., A. Yin, J. Xu, and J. M. Valles, Superconducting pair correlations in an amorphous insulating nanohoneycomb film, Science **318**, 1273 (2007).

[9] B. Sacépé, C. Chapelier, T. I. Baturina, V. M. Vinokur, M. R. Baklanov, and M. Sanquer, Disorder-Induced Inhomogeneities of the Superconducting State Close to the Superconductor-Insulator Transition, Phys. Rev. Lett. **101**, 157006 (2008).

[10] C. A. Marrache-Kikuchi, H. Aubin, A. Pourret, K. Behnia, J. Lesueur, L. Bergé, and L. Dumoulin, Thickness-tuned superconductor-insulator transitions under magnetic field in ***a***-NbSi, Phys. Rev. B **78**, 144520 (2008).

[11] S. M. Hollen, H. Q. Nguyen, E. Rudisaile, M. D. Stewart, Jr., J. Shainline, J. M. Xu, and J. M. Valles, Jr., Cooper-pair insulator phase in superconducting amorphous bi films induced by nanometer-scale thickness variations, Phys. Rev. B **84**, 064528 (2011).

[12] S. V. Postolova, A. Y. Mironov, M. R. Baklanov, V. M. Vinokur, and T. I. Baturina, Reentrant resistive behavior and dimensional crossover in disordered superconducting tin films, Sci. Rep. **7**, 1718 (2017).

[13] T. I. Baturina, V. Vinokur, A. Y. Mironov, N. Chtchelkatchev, D. Nasimov, and A. Latyshev, Nanopattern-stimulated superconductor-insulator transition in thin tin films, Europhys. Lett. **93**, 47002 (2011).

[14] S. Poran, T. Nguyen-Duc, A. Auerbach, N. Dupuis, A. Frydman, and O. Bourgeois, Quantum criticality at the superconductor-insulator transition revealed by specific heat measurements, Nat. Commun. **8**, 14464 (2017).

[15] D. Shahar and Z. Ovadyahu, Superconductivity near the mobility edge, Phys. Rev. B **46**, 10917 (1992).

[16] B. Sacépé, T. Dubouchet, C. Chapelier, M. Sanquer, M. Ovadia, D. Shahar, M. Feigel'Man, and L. Ioffe, Localization of preformed Cooper pairs in disordered superconductors, Nat. Phys. **7**, 239 (2011).

[17] S. Poran, E. Shimshoni, and A. Frydman, Disorder-induced superconducting ratchet effect in nanowires, Phys. Rev. B **84**, 014529 (2011).

[18] A. Roy, E. Shimshoni, and A. Frydman, Quantum Criticality at the Superconductor-Insulator Transition Probed by the Nernst Effect, Phys. Rev. Lett. **121**, 047003 (2018).

[19] M. A. Paalanen, A. F. Hebard, and R. R. Ruel, Low-Temperature Insulating Phases of Uniformly Disordered Two-Dimensional Superconductors, Phys. Rev. Lett. **69**, 1604 (1992).

[20] A. Yazdani and A. Kapitulnik, Superconducting-Insulating Transition in Two-Dimensional a-MoGe Thin Films, Phys. Rev. Lett. **74**, 3037 (1995).

[21] V. Gantmakher, M. Golubkov, V. Dolgopolov, G. Tsydynzhapov, and A. Shashkin, Destruction of localized electron pairs above the magnetic-field-driven superconductor-insulator transition in amorphous In-O films, JETP Lett. **68**, 363 (1998).

[22] G. Sambandamurthy, L. W. Engel, A. Johansson, and D. Shahar, Superconductivity-Related Insulating Behavior, Phys. Rev. Lett. **92**, 107005 (2004).

[23] G. Sambandamurthy, L. W. Engel, A. Johansson, E. Peled, and D. Shahar, Experimental Evidence for a Collective Insulating State in Two-Dimensional Superconductors, Phys. Rev. Lett. **94**, 017003 (2005).

[24] M. A. Steiner, G. Boebinger, and A. Kapitulnik, Possible Field-Tuned Superconductor-Insulator Transition in High-T_c Superconductors: Implications for Pairing at High Magnetic Fields, Phys. Rev. Lett. **94**, 107008 (2005).

[25] T. Baturina, J. Bentner, C. Strunk, M. Baklanov, and A. Satta, From quantum corrections to magnetic-field-tuned superconductor–insulator quantum phase transition in tin films, Phys. B: Condens. Matter **359-361**, 500 (2005).

[26] T. I. Baturina, C. Strunk, M. R. Baklanov, and A. Satta, Quantum Metallicity on the High-Field Side of the Superconductor-Insulator Transition, Phys. Rev. Lett. **98**, 127003 (2007).

[27] R. W. Crane, N. P. Armitage, A. Johansson, G. Sambandamurthy, D. Shahar, and G. Grüner, Fluctuations, dissipation, and nonuniversal superfluid jumps in two-dimensional superconductors, Phys. Rev. B **75**, 094506 (2007).

[28] V. M. Vinokur, T. I. Baturina, M. V. Fistul, A. Y. Mironov, M. R. Baklanov, and C. Strunk, Superinsulator and quantum synchronization, Nature (London) **452**, 613 (2008).

[29] R. Ganguly, I. Roy, A. Banerjee, H. Singh, A. Ghosal, and P. Raychaudhuri, Magnetic field induced emergent inhomogeneity in a superconducting film with weak and homogeneous disorder, Phys. Rev. B **96**, 054509 (2017).

[30] M. Mondal, A. Kamlapure, M. Chand, G. Saraswat, S. Kumar, J. Jesudasan, L. Benfatto, V. Tripathi, and P. Raychaudhuri, Phase Fluctuations in a Strongly Disordered *s*-Wave NbN Superconductor Close to the Metal-Insulator Transition, Phys. Rev. Lett. **106**, 047001 (2011).

[31] K. A. Parendo, K. H. S. B. Tan, A. Bhattacharya, M. Eblen-Zayas, N. E. Staley, and A. M. Goldman, Electrostatic Tuning of the Superconductor-Insulator Transition in Two Dimensions, Phys. Rev. Lett. **94**, 197004 (2005).

[32] A. Caviglia, S. Gariglio, N. Reyren, D. Jaccard, T. Schneider, M. Gabay, S. Thiel, G. Hammerl, J. Mannhart, and J.-M. Triscone, Electric field control of the $LaAlO_3/SrTiO_3$ interface ground state, Nature (London) **456**, 624 (2008).

[33] R. Cohen, M. Nikolaevsky, R. Salem, and A. Frydman, Setup for pressurizing thin films through the superconductor–insulator transition, Rev. Sci. Instrum. **92**, 083903 (2021).

[34] A. M. Goldman and N. Marković, Superconductor-insulator transitions in the two-dimensional limit, Physics Today **51**, 39 (1998).

[35] Y.-H. Lin, J. Nelson, and A. Goldman, Superconductivity of very thin films: The superconductor–insulator transition, Physica C **514**, 130 (2015).

[36] S. Sachdev, Quantum phase transitions, *Handbook of Magnetism and Advanced Magnetic Materials* (Wiley, New York, 2007).

[37] A. Ghosal, M. Randeria, and N. Trivedi, Role of Spatial Amplitude Fluctuations in Highly Disordered *s*-Wave Superconductors, Phys. Rev. Lett. **81**, 3940 (1998).

[38] A. Ghosal, M. Randeria, and N. Trivedi, Inhomogeneous pairing in highly disordered *s*-wave superconductors, Phys. Rev. B **65**, 014501 (2001).

[39] K. Bouadim, Y. L. Loh, M. Randeria, and N. Trivedi, Single-and two-particle energy gaps across the disorder-driven superconductor–insulator transition, Nat. Phys. **7**, 884 (2011).

[40] D. Dentelski, A. Frydman, E. Shimshoni, and E. G. Dalla Torre, Tunneling probe of fluctuating superconductivity in disordered thin films, Phys. Rev. B **97**, 100503(R) (2018).

[41] D. Sherman, G. Kopnov, D. Shahar, and A. Frydman, Measurement of a Superconducting Energy Gap in a Homogeneously Amorphous Insulator, Phys. Rev. Lett. **108**, 177006 (2012).

[42] A. Kamlapure, T. Das, S. C. Ganguli, J. B. Parmar, S. Bhattacharyya, and P. Raychaudhuri, Emergence of nanoscale inhomogeneity in the superconducting state of a homogeneously disordered conventional superconductor, Sci. Rep. **3**, 2979 (2013).

[43] G. Kopnov, O. Cohen, M. Ovadia, K. H. Lee, C. C. Wong, and D. Shahar, Little-Parks Oscillations in an Insulator, Phys. Rev. Lett. **109**, 167002 (2012).

[44] P. G. De Gennes, Boundary effects in superconductors, Rev. Mod. Phys. **36**, 225 (1964).

[45] G. Deutscher and P. G. de Gennes, *in Superconductivity*, edited by R. D. Parks (Taylor and Francis, London, 1969).

[46] L. Merchant, J. Ostrick, R. P. Barber, Jr., and R. C. Dynes, Crossover from phase fluctuation to amplitude-dominated superconductivity: A model system, Phys. Rev. B **63**, 134508 (2001).

[47] A. Frydman and R. Dynes, Granular superconductors and ferromagnets: A proximity-effect-based analogue, Philos. Mag. B **81**, 1153 (2001).

[48] Z. Ovadyahu, Some finite temperature aspects of the anderson transition, J. Phys. C **19**, 5187 (1986).

[49] U. Givan and Z. Ovadyahu, Compositional disorder and transport peculiarities in the amorphous indium oxides, Phys. Rev. B **86**, 165101 (2012).

[50] D. Kowal and Z. Ovadyahu, Disorder induced granularity in an amorphous superconductor, Solid State Commun. **90**, 783 (1994).

[51] T. I. Baturina, A. Y. Mironov, V. M. Vinokur, M. R. Baklanov, and C. Strunk, Localized Superconductivity in the Quantum-Critical Region of the Disorder-Driven Superconductor-Insulator Transition in TiN Thin Films, Phys. Rev. Lett. **99**, 257003 (2007).

[52] T. I. Baturina, A. Y. Mironov, V. Vinokur, M. Baklanov, and C. Strunk, Hyperactivated resistance in tin films on the insulating side of the disorder-driven superconductor-insulator transition, JETP Lett. **88**, 752 (2008).

[53] V. Humbert, M. Ortuño, A. Somoza, L. Bergé, L. Dumoulin, and C. Marrache-Kikuchi, Overactivated transport in the localized phase of the superconductor-insulator transition, Nat. Commun. **12**, 6733 (2021).

[54] Y. Dubi, Y. Meir, and Y. Avishai, Theory of the magnetoresistance of disordered superconducting films, Phys. Rev. B **73**, 054509 (2006).

[55] Y. Dubi, Y. Meir, and Y. Avishai, Nature of the superconductor–insulator transition in disordered superconductors, Nature (London) **449**, 876 (2007).

[56] B. L. Altshuler and A. G. Aronov, Electron–electron interaction in disordered conductors, in *Modern Problems in Condensed Matter Sciences* (Elsevier, Amsterdam, 1985), Vol. 10, pp. 1–153.